chemistry proceedings

Proceedings

UV-LED Photocatalytic Device for the Oxidation of Ethanol and Hexane Vapors in Air

Catherine B. Almquist[1], Isabelle O'Hare[1], Linda Garza[1], Akram Badahman[1], Will Jung[1], Samantha Hanzel[1] and John Neal[1]

[1]Chemical, Paper, Biomedical Engineering Department, Miami University, Oxford, Ohio 45056 ; almquic@miamioh.edu; ohareim@miamioh.edu; garzalk@miamioh.edu; badahmas@miamioh.edu; jungwr2@miamioh.edu; hanzelsc@miamioh.edu; nealjj3@miamioh.edu

Abstract: An annulus-type of photocatalytic reactor was designed, constructed, and characterized for its performance for the oxidation of ethanol and hexane vapors in air. The photocatalytic device utilized ultraviolet (λ=365 nm) light emitting diodes (UV-LEDs) as light sources and photocatalytic (Degussa P25 TiO_2) films coated on the inside surfaces of the reactor. These reactor systems can be applied to mobile and niche applications. UV-LEDs are small, robust light sources that require low direct current (DC) power, which could be provided by a battery. The study results demonstrate that the UV-LED-based photocatalytic system is capable of reducing or eliminating ethanol and hexane vapors in air. Test results have demonstrated the sensitivity of the effectiveness of the UV-LED-based photocatalytic system on operating parameters, including flow rate, concentration, type of VOC, humidity, and longevity.

Introduction

The motivation for this study was to develop a device that can oxidize volatile organic carbon compounds (VOCs), such as fuel vapors, in mobile applications. For example, the development of a mobile UV-LED photocatalytic oxidation system to reduce evaporative fuel vapor emissions from automobiles will significantly improve urban air quality. The improvement of urban ambient air quality will reduce detrimental health impacts of urban air pollutants. Therefore, such a device has potential to enhance economic opportunity and human health.

The United States Environmental Protection Agency (US EPA) has had a priority to reduce urban air toxics since 1990, when the Clean Air Act Amendments were passed [1]. Although much progress has been made to reduce hazardous air pollutants, additional work still needs to be done, particularly in urban areas with high traffic density. People who live in urban centers have greater exposure to air pollutants due to the greater number of and proximity to both stationary and mobile sources of air pollution, and therefore, they have a greater risk of detrimental health impacts due to air pollution. According to an EPA website, "Low-income neighborhoods, tribal populations and communities of color that live in urban areas may be disproportionately exposed to air pollution, which is a barrier to economic opportunity and security" [2].

The transportation sector was the source of 1.4 million tons of VOC air emissions in the US in 2020 [3]. Although much has been done to reduce the emissions of VOCs from automobiles, more must be done to prevent the degradation of air quality in urban centers.

There are four major ways in which fuel vapors are emitted from the automobile: 1) through diurnal evaporation, which is the evaporation of fuels during daylight hours when the fuel is heated and thus more volatile by an increase in ambient temperature, 2) through operating losses, which result from fuel volatilization and permeation of fuels through hoses as the temperature of the engine and exhaust system increase during operation, 3) from "hot soak", which occurs from fuel volatilization due to radiant heat from the engine after the engine is turned off, and 4) through refueling, during which fuel vapors in the gas tank are displaced with liquid fuel, thus venting the fuel vapors from the fuel tank [4].

Since approximately 1998, automobiles in the US have been equipped with onboard refueling vapor recovery (ORVR) systems to reduce the evaporative fuel vapor emissions, achieving a 98% reduction of evaporative fuel vapors compared to uncontrolled evaporative emissions. The ORVR system works by directing fuel vapors from the gas tank to a carbon canister. The activated carbon in the carbon canister adsorbs the fuel vapors. Then, when the automobile is turned on, a control system allows the carbon canister to be purged with air, and the purged vapors and air are directed to the engine, where the vapors are burned [5].

Adsorbents, such as activated carbon, have finite amounts of adsorption capacity for fuel vapors, and the adsorption capacity is dependent upon both type of fuel vapors and adsorbent temperature. As temperature increases, the adsorption capacity decreases. Thus, when the temperature of the adsorbent increases (e.g. during diurnal temperature swings), the adsorbed fuel vapors desorb from the activated carbon and are emitted to the environment. These emissions are evaporative fuel vapor emissions. Evaporative fuel vapor emissions standards have been set on all light duty vehicles and trucks from 2004 to the present, and more stringent regulations are to be implemented worldwide, especially within the US [6].

A relatively new challenge for evaporative fuel emissions control is the advent of flex fuel vehicles. Flex fuel vehicles can operate with different fuels having different volatilities. This makes evaporative fuel emissions control difficult, since different fuels will behave differently with temperature, and the activated carbon will have different adsorption capacities for different types of fuel [7].

In this project, ethanol and hexane vapors were used as representative VOCs to demonstrate the performance of the UV LED photocatalytic devices for potential application as evaporative fuel vapor emission control. Ethanol is blended with gasoline at ratios from 10 vol% to 85 vol% [8], which motivated the use of ethanol as a representative fuel vapor. Hexane is a representative alkane that is contained in gasoline. The performance of the devices was assessed as functions of VOC concentration, residence time, and longevity. Preliminary data was also obtained as functions of UV LED wavelength and humidity in the inlet air stream.

Experimental Methods

Materials

Hexane and ethanol were purchased from Fisher Scientific and were used as received. Titanium dioxide (TiO_2) P25 was purchased from Evonik and used as received.

Reactors

Two identical UV LED photocatalytic devices were designed and fabricated from 5 cm x 5 cm x 16.5 cm length block aluminum, and two additional devices were constructed exactly the same as the first two but half the length (8.25 cm length). Using the block aluminum as a base, a 3 cm diameter cylindrical opening was drilled into the block aluminum to form the outer diameter of the cylindrical reactor. A 1.9 cm diameter aluminum rod was used to form the inner diameter of the annulus reactor. The photocatalytic film was placed on the aluminum rod, while the UV-LEDs were placed on the inside wall of the cylindrical core of the reactor. For the "long" reactors, the illuminated surface area of the photocatalytic film is 91 cm^2, while the open volume of the reactor (without UV LEDs) is 77 cm^3. The "small" reactors are half the length of the "long" reactors, but otherwise they have the same design. Figure 1a-c show pictures of the "long" and "short" reactors.

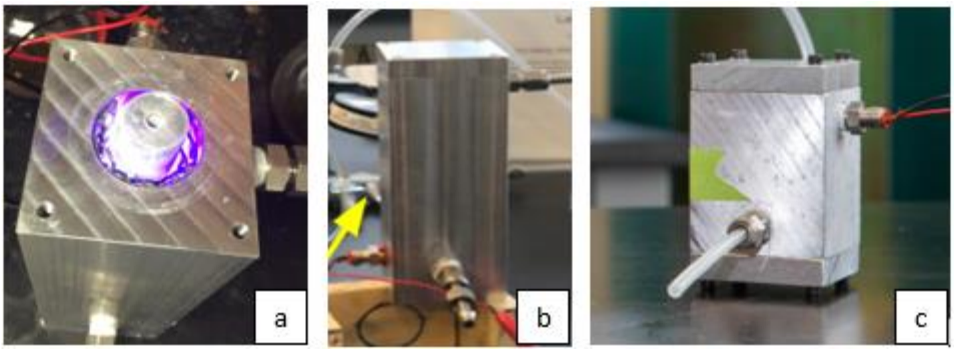

Figure 1. Photographs of the prototype devices: a) Inside view of the annulus reactor with top removed; b) long reactor; c) short reactor.

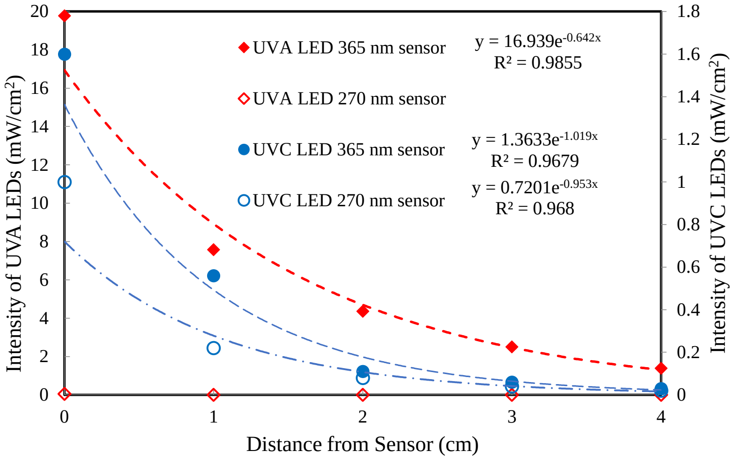

Figure 2. Comparison of UVA and UVC LEDs: light intensity.

Both "long" reactors and one "short" reactor contain UVA LEDs from Waveform lighting [9]. These LEDs have a predominant output at 365 nm wavelength. The power required for the "long" reactors is 12 W, whereas the short reactor power is 6 W. The second "short" reactor has UVC LEDs, also from Waveform lighting [10]. The output of the UVC LEDs center at wavelengths near 275 nm. However, the UVC LEDs have much lower light intensity (mW/cm^2) than the UVA LEDs, as shown in Figure 2. The light intensity measurements were conducted with an Omega light meter that has 2 light sensors: a sensor centered at 365 nm wavelengths and a sensor centered at 270 nm wavelength. While the UVC LEDs had energy at 270 nm, the light intensity was more than an order of magnitude lower than that of the UVA LEDs.

Photocatalytic films

Degussa P25 TiO_2, a commercially-available photocatalyst, was used for all photocatalytic films in this study. The BET surface area of P25 TiO_2 photocatalyst powder was measured to be 50 m^2/g using nitrogen adsorption at 77 K on a Micromeritics TriStar surface area analyzer. In addition, the bandgap of P25 TiO_2 was measured to be 3.05 eV using Tauc plots with data obtained from diffuse reflectance analyses on a Perkin Elmer Lambda 750 model UV/Vis/NIR spectrometer. The TiO_2 films were prepared on aluminum rods, which formed the center of the reactor, by a dip-coating method. The aluminum rods were prepared first by using sandpaper to roughen the surface of the aluminum rod. The rods were then heated to 500 C to form a thin aluminum oxide layer on the aluminum rod. Finally, a slurry of TiO_2 in ethanol was prepared. The aluminum rod was heated to approximately 60 C and dipped into the ethanol slurry to coat the aluminum rod with TiO_2. The heat quickly drives the solvent from the rod, leaving behind a relatively even and smooth coating of TiO_2 photocatalyst. The coated aluminum rod is then heated again to approximately 60 C to dry and remove residual solvent from the coating. Figure 3 shows a TiO_2-coated aluminum rod used in our prototype devices.

Figure 3. TiO_2-coated aluminum rod used within the current prototype devices.

The mass of TiO_2 on the rod can significantly impact the photocatalytic film durability and performance. If the film is too thick, the film will readily flake off from the rod, which will significantly impact its performance in the photocatalytic oxidation of organic vapors. Therefore, the photocatalytic films used in this study had masses of approximately 1.5 mg /cm^2 of illuminated surface area.

Test system

The test apparatus used for this study is shown schematically in Figure 4. Mass flow controllers (0-100 sccpm) were used to control air flow rates through the test systems at flow rates of 25 ccpm, 50 ccpm, and 100 ccpm. Lab-made diffusion cells were used to generate ethanol and hexane vapor challenges to the reactors over a wide range of concentrations, depending upon the path length and diameter of the diffusion paths. Samples were collected from the reactor effluents either using gas tight syringes for instantaneous samples or using gas sampling bags to collect composite samples over 10 to 20 minutes. The samples from both the inlets and outlets of the reactors were taken and analyzed using an Agilent 5890 gas chromatograph with a flame ionization detector (GC/FID). The GC/FID was used to quantify ethanol, acetaldehyde (a partial oxidation product of ethanol), and hexane vapor concentrations. The GC column was an HP-5. Gas injections (250 uL) were made using a gas-tight syringe. Calibration standards were prepared using 1-liter gas sampling bags, and the GC/FID was calibrated for ethanol, acetaldehyde and hexane vapor. CO_2 was measured in selected studies using a calibrated Amprobe CO_2 meter.

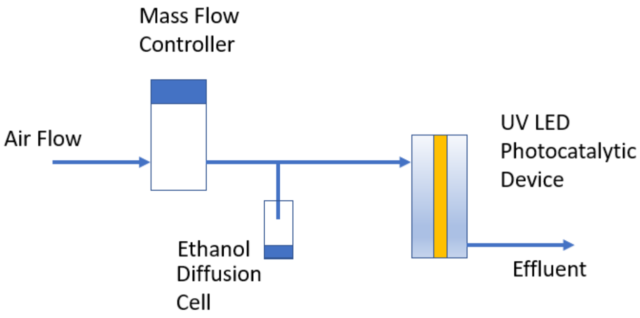

Figure 4. Schematic of test system.

Fourier transform infrared analyses (FTIR analyses, Nicolet 670 FTIR, Thermo Electron Corporation) were conducted on the TiO_2 photocatalytic films to characterize organic functional groups remaining on the photocatalyst after several days of operation in the UV LED photocatalytic devices.

Results and Discussion

Ethanol vapor photocatalytic oxidation

Ethanol photocatalytic oxidation has been studied by many researchers [11-18]. Generally, the photocatalytic oxidation of ethanol initially leads to acetaldehyde, and ultimately to carbon dioxide [11-18]. Acetaldehyde is the predominant by-product observed in the GC/FID analyses, however, acetic acid, formic acid, and formaldehyde have also been observed and are incorporated into publish mechanisms for the gas-phase photocatalytic oxidation of ethanol [11-18].

In the UVA-LED test systems (both “short” and “long” reactors), ethanol was > 98% oxidized under all conditions studied. The ethanol challenge concentrations ranged from 175 ppm to 500 ppm, and the residence times of the gas flow in the UV LED photocatalytic devices ranged from 40 seconds to 90 seconds. The total hydrocarbon conversions, which include all trace peaks observed in the reactor effluent (ethanol, acetaldehyde, formaldehyde, and acetic acid), were greater than 90% for all trials when operating for less than one week continuously.

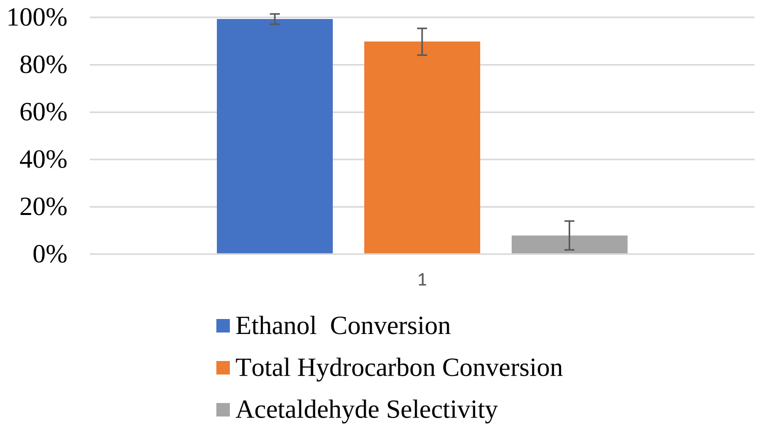

Figure 5. Summary of ethanol photocatalytic oxidation experiments with continuous operation for up to three weeks.

When the devices are left onstream for more than a week, the presence of acetaldehyde in the reactor effluent is observed. After three weeks of continuous operation with an ethanol challenge of approximately 300 ppm and a residence time of 80 seconds, the ethanol conversion in the UV LED device was still > 98%, but the selectivity to acetaldehyde increased from < 2% to approximately 10%. Figure 5 graphically shows the experimental results after the device has been in continuous operation for two weeks.

One reason that the performance of the UV LED photocatalytic device appears to degrade slightly over time is due to partial oxidation by-products building up on the photocatalytic film in the device. This is supported by Coronado, et al [13] and by Piera, et al [14], who observed a buildup of acetate and formate complexes on TiO2 photocatalysts. In an effort to characterize the used photocatalyst, FTIR analyses were conducted on unused and used photocatalysts. Figure 6 shows a comparison of the FTIR analyses of used and unused P25 TiO_2. It is shown that the used catalysts, after 14 days of continuous operation, contains organic functional groups characteristic of aldehydes and alkenes.

Figure 6. FTIR analyses of P25 unused and used under continuous operation for 14 days.

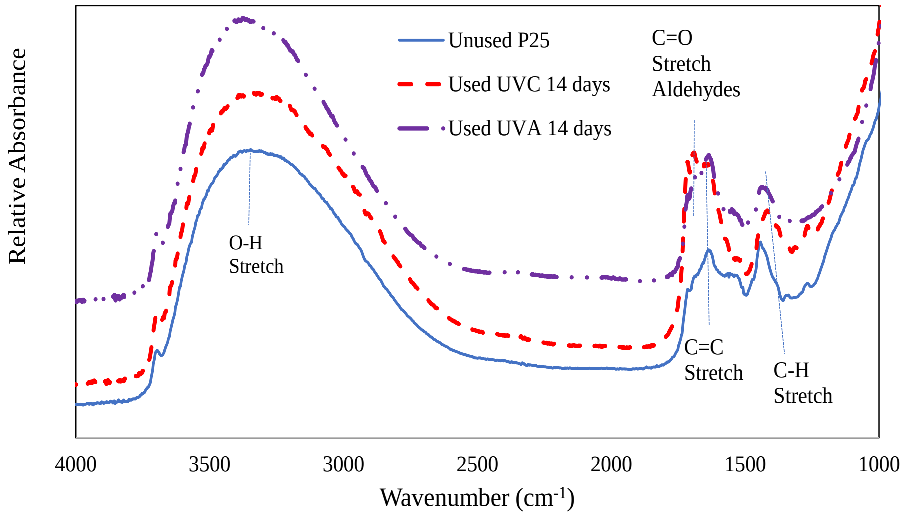

Figure 6. FTIR analyses of P25 unused and used under continuous operation for 14 days.

For the short UVC reactor, ~30% conversion of ethanol was observed with ~40% selectivity to acetaldehyde and ~30% selectivity of acetic acid, with the remainder 30% presumably to CO_2. At low light intensities, low ethanol conversions were observed, which leads to the formation of acetaldehyde and acetic acid. This observation is supported by published mechanisms for ethanol vapor photocatalytic oxidation [15-18].

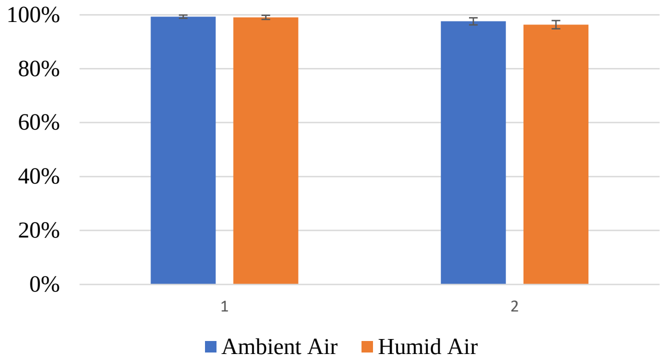

Figure 7. Comparison of UVA-LED photocatalytic oxidation of ethanol vapor. The influent air was house air and humidified house air.

The effect of humidity on the photocatalytic oxidation of ethanol in the UV LED device was investigated. Additional humidity was added to experimental trials by adding a water-filled bubbler to the inlet air line prior to the ethanol vapor diffusion cell. The additional humidity did not appear to impact the performance of the device significantly, as shown in Figure 7. However, the acetaldehyde selectivity increased from 0.2% to 1.2%. In studies by Sola, et al [11], water vapor depressed the photocatalytic oxidation of ethanol by competing with the ethanol for adsorption sites.

Hexane vapor photocatalytic oxidation

Studies to investigate the photocatalytic oxidation of hexane vapor have been published [19-21]. While Saucedo-Lucero and Arriaga [19] have reported hexanol and hexanone as partial oxidation products, other studies reported that the partial oxidation products of hexane vapor were not detectable in the gas phase by GC/FID [20,21]. In this study, partial oxidation products of hexane were not observed. It is likely that the partial oxidation products of hexane adhere to the surface of the photocatalyst until deeply oxidized to carbon dioxide.

In the UVA-LED "long" test systems, the hexane vapor was introduced into the devices over a range of concentrations and flow rates. When combining the experimental data from the "long" UVA LED reactor systems, the photocatalytic oxidation of hexane vapor followed Langmuir-Hinshelwood trends, as shown in Figure 8. This is supported by the published literature [19-21], in which the photocatalytic oxidation of hexane vapors were also modeled according to the Langmuir-Hinshelwood equation. The solid line in Figure 8 was fit to the experimental data using the Langmuir-Hinshelwood model (Equation 1) and the sum of least squares method.

$$-r_A = -\frac{dC_A}{dt} = \frac{k\,K\,C_A}{1+K\,C_A} \qquad (1)$$

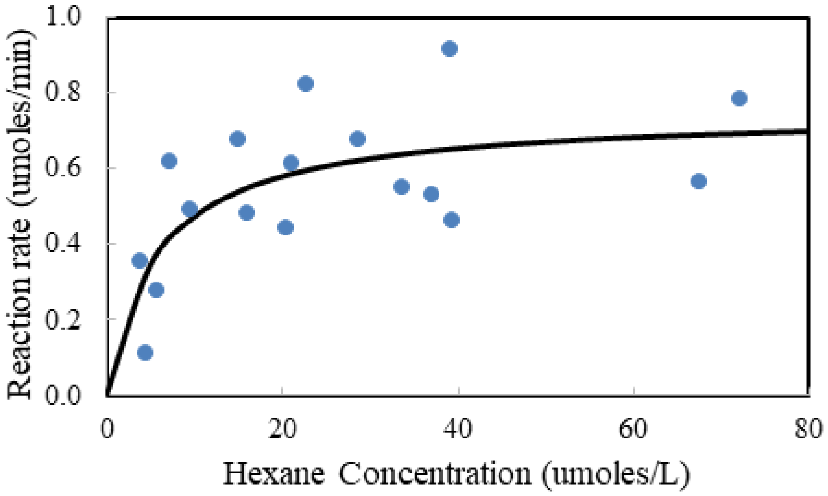

Figure 8. Summary of hexane vapor photocatalytic oxidation in UVA LED "long" reactors, modeleding using Langmuir-Hinshelwood kinetics.

In equation 1, $-r_A = - dC_A/dt$ is the rate of reaction of hexane vapor (umoles L^{-1} min^{-1}); k is the rate of reaction at maximum coverage of the catalyst with hexane vapor (umoles L^{-1} min^{-1}), and K is the equilibrium constant for adsorption of hexane onto the catalyst (L $umole^{-1}$). In this study, the model parameters that best fit the experimental data were k = 0.75 umoles L^{-1} min^{-1}, and K = 0.17 L $umole^{-1}$.

In these trials, the residence times of hexane vapor in the photocatalytic device ranged from 40 seconds to 170 seconds, and the hexane concentrations ranged from 100 ppm to 2000 ppm. In selected trials, the carbon dioxide concentration was measured using an Amprobe CO_2 meter. The carbon balances in those trials averaged near 100%, where the carbon contained in the hexane vapor and CO_2 in the effluent was approximately equal to the carbon input with hexane to the device.

One of the "long" UVA LED photocatalytic devices was operated continuously for one month. There was no observed degradation in performance of the device.

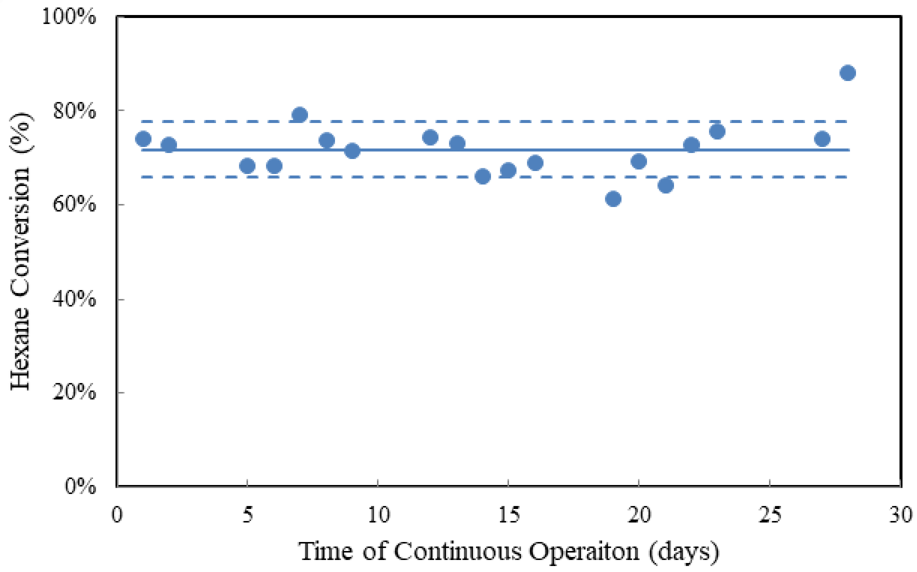

Figure 9. Summary of test results for a UV LED "long" device operating continuously for 1 month. The hexane concentration was approximately 380 ppm, and the residence time was 65 seconds.

In an effort to characterize the used photocatalyst, FTIR analyses were conducted on unused and used photocatalysts. Figure 10 shows a comparison of the FTIR analyses of used and unused P25 TiO_2. It is shown that the used catalysts, after 28 days of continuous operation, contains organic functional groups characteristic of aldehydes and alkenes.

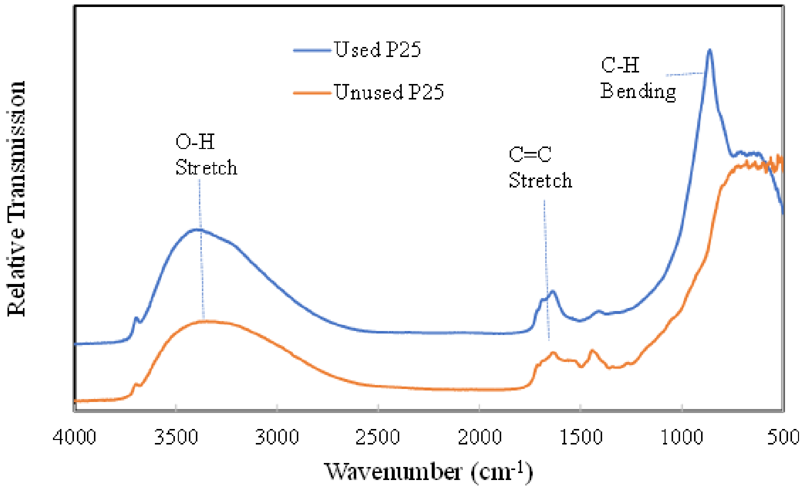

Figure 10. FTIR analyses to compare used and unused P25 TiO2. The used catalyst was from a device continuously operated for 28 days with hexane vapor at 380 ppm.

The effects of humidity on the photocatalytic oxidation of hexane vapors was assessed. Humidity was generated by saturating the air with water vapor using a bubbler-type vapor generator prior to the hexane vapor diffusion cell. The relative humidity in the compressed house air was 18%, whereas the relative humidity of the humidified house air was 78%. The humidity lowered the conversion of hexane vapor by 4%-6%. The water vapor likely competed for adsorption sites on the catalyst, thus lowering the observed conversion of hexane vapors in the device.

Conclusion

Small mobile UV-LED photocatalytic devices were designed, fabricated, and demonstrated as effective tools to reduce or eliminate volatile organic compounds from air. The devices, which require ~12 W of direct current power, were able to oxidize >98% of ethanol vapors over a range of concentrations from 175 ppm to 500 ppm at residence times ranging from 40 s to 170 s. Additionally, the devices were able to degrade hexane vapors by > 60% at concentrations ranging from 100 ppm to nearly 2000 ppm. Very little degradation of performance was observed after a month of continuous operation. Upon further analyses of the used photocatalysts, there was some evidence of hydrocarbon build-up, as indicated by FTIR analyses. The performance of the devices were only slightly hindered when operating at ~80% relative humidity, likely due to competitive adsorption of water vapor with the organic vapor on the catalyst surface.

Upon further development, UV LED photocatalytic devices can fulfill niche mobile applications, for example, evaporative fuel vapor emissions control.

Funding: “This article was developed under Assistance Agreement No . SV-84001601-0 awarded by the U.S. Environmental Protection Agency to Miami University. It has not been formally reviewed by the US EPA. The views expressed in this document are solely those of the authors of this article and do not necessarily reflect those of the Agency. EPA does not endorse any products or commercial services mentioned in this publication.

Acknowledgments: The authors would like to acknowledge Miami’s Instrumentation Lab, who machined the photocatalytic devices, and Stant Manufacturing, Inc. in Connorsville, Indiana for providing the authors motivation for this project.

Conflicts of Interest: The authors declare no conflict of interest.

References

[1] https://www.epa.gov/urban-air-toxics , accessed on September 10, 2021.
[2] https://www.epa.gov/urban-air-toxics/about-urban-air-toxics , accessed on September 10, 2021.
[3] https://www.statista.com/statistics/1234976/road-transportation-volatile-organic-compounds-emissions-us/, accessed on September 10, 2021.
[4] http://tiij.org/issues/issues/5_1/5_1e/5_1e.html , accessed on September 10, 2021.
[5] https://en.wikipedia.org/wiki/Onboard_refueling_vapor_recovery , accessed on September 10, 2021.
[6] https://www.automotive-iq.com/exhaust/articles/evaporative-emission-regulations-and-evap-systems
[7] Siciliano, B., Martins da Silva, C., Loureiro, L.N., Vicentini, P.C., and Arbilla, G. (2021). Hydrocarbon emissions in flex fuel vehicles using ethanol: Preliminary results using a method implemented in Brazil. Fuel, 287,119506. https://doi.org/10.1016/j.fuel.2020.119506.
[8] https://afdc.energy.gov/fuels/ethanol_blends.html, accessed on September 10, 2021.
[9] https://www.waveformlighting.com/datasheets/CS_7021.pdf

[10] https://www.waveformlighting.com/datasheets/CS_7026.pdf

[11] Sola, A.C., Garzón Sousa, D., Araña, J., González Díaz, O., Doña Rodríguez, J.M., Ramírez de la Piscina, P., and Homs, N. (2016). Differences in the vapour phase photocatalytic degradation of ammonia and ethanol in the presence of water as a function of TiO2 characteristics and the presence of O2. Catalysis Today, 266, pp. 53-61. https://doi.org/10.1016/j.cattod.2015.08.008.

[12] Kolinko, P.A., Selishchev, D.S. & Kozlov, D.V. (2015). Visible Light Photocatalytic Oxidation of Ethanol Vapor on Titanium Dioxide Modified with Noble Metals. *Theoretical and Experimental Chemistry*, **51, pp.** 96–103 (2015). https://doi.org/10.1007/s11237-015-9402-1

[13] Coronado, J.M., Kataoka, S., Tejedor-Tejedor, I., and Anderson, M.A. (2003). Dynamic phenomena during the photocatalytic oxidation of ethanol and acetone over nanocrystalline TiO2: simultaneous FTIR analysis of gas and surface species. Journal of Catalysis, 219 (1), pp. 219-230. https://doi.org/10.1016/S0021-9517(03)00199-4.

[14] Piera, E., Ayllón, J.A., Doménech, X., and Peral, J. (2002). TiO_2 deactivation during gas-phase photocatalytic oxidation of ethanol. Catalysis Today, 76 (2–4), pp. 259-270. https://doi.org/10.1016/S0920-5861(02)00224-9.

[15] Sauer, M.L. and Ollis, D. F. (1996). Photocatalyzed oxidation of ethanol and acetaldehyde in humidified air. Journal of Catalysis, 158, pp. 570-582.

[16] Nimlos, M.R., Wolfrum, E.J., Brewer, M.L., Fennell, J.A., and Bintner, G. (1996). Gas-phase heterogeneous photocatalytic oxidation of ethanol: Patheways and kinetic modeling. Environmental Science and Technology, 30, pp. 3102-3110.

[17] Muggli, D.S., McCue, J.T., and Falconer, J.L. (1998). Mechanism of the Photocatalytic Oxidation of Ethanol on TiO2. Journal of Catalysis, 173(2), pp. 470-483. https://doi.org/10.1006/jcat.1997.1946.

[18] Takeuchi, M., Deguchi, J., Sakai, S., and Anpo, M. (2010). Effect of H2O vapor addition on the photocatalytic oxidation of ethanol, acetaldehyde and acetic acid in the gas phase on TiO2 semiconductor powders. Applied Catalysis B: Environmental, 96 (1–2), pp. 218-223. https://doi.org/10.1016/j.apcatb.2010.02.024.

[19] Saucedo-Lucero, J.O., and Arriaga, S. (2013). Photocatalytic degradation of hexane vapors in batch and continuous systems using impregnated ZnO nanoparticles. Chemical Engineering Journal, 218, pp. 358-367. https://doi.org/10.1016/j.cej.2012.12.050.

[20] Boulamanti, A.K., and Philippopoulos, C.J. (2009). Photocatalytic degradation of C5–C7 alkanes in the gas–phase. Atmospheric Environment, 43(20), pp. 3168-3174. https://doi.org/10.1016/j.atmosenv.2009.03.036.

[21] Zhang, P. and Liu, J. (2004). Photocatalytic degradation of trace hexane in the gas phase with and without ozone addition: kinetic study. Journal of Photochemistry and Photobiology A: Chemistry, 167 (2–3), pp. 87-94. https://doi.org/10.1016/j.jphotochem.2004.05.015.